Estimation of radiation dose-reduction factor for cerium oxide nanoparticles in MRC-5 human lung fibroblastic cells and MCF-7 breast-cancer cells

Nouraddin Abdi Goushbolagh, Razzagh Abedi Firouzjah, Kourosh Ebrahimnejad Gorji, Mohammadjavad Khosravanipour, Saman Moradi, Amin Banaei, Akram Astani, Masoud Najafi, Mohammad Hosein Zare & Bagher Farhood

Published online: 27 Nov 2018.

Submit your article to this journal

View Crossmark data

Taylor & Francis
Taylor & Francis Group

Check for updates

Estimation of radiation dose-reduction factor for cerium oxide nanoparticles in MRC-5 human lung fibroblastic cells and MCF-7 breast-cancer cells

Nouraddin Abdi Goushbolagh[a], Razzagh Abedi Firouzjah[b], Kourosh Ebrahimnejad Gorji[b], Mohammadjavad Khosravanipour[c], Saman Moradi[c], Amin Banaei[c], Akram Astani[d,e], Masoud Najafi[f], Mohammad Hosein Zare[a,g] and Bagher Farhood[h]

[a]Department of Medical Physics, Faculty of Medicine, Shahid Sadoughi University of Medical Sciences, Yazd, Iran; [b]Department of Medical Physics Radiobiology and Radiation Protection, Babol University of Medical Sciences, Babol, Iran; [c]Department of Medical Physics, Faculty of Medical Sciences, Tarbiat Modares University, Tehran, Iran; [d]Zoonotic Diseases Research Center, School of public health, Shahid Sadoughi University of Medical Sciences, Yazd, Iran; [e]Department of Microbiology, Faculty of Medical sciences, Shahid Sadoughi University of Medical Sciences, Yazd, Iran; [f]Radiology and Nuclear Medicine Department, School of Paramedical Sciences, Kermanshah University of Medical Sciences, Kermanshah, Iran; [g]Radiotherapy Research Center, Shahid Sadoughi University of Medical Sciences, Yazd, Iran; [h]Departments of Medical Physics and Radiology, Faculty of Paramedical Sciences, Kashan University of Medical Sciences, Kashan, Iran

ABSTRACT

In the current study, radiation dose-reduction factor (DRF) of nanoceria or cerium oxide nanoparticles (CONPs) in MRC-5 Human Lung Fibroblastic Cells and MCF-7 Breast-Cancer Cells was estimated. Characterization of CONPs was determined using scanner electron microscope (SEM), energy dispersive spectroscopy (EDS), transmission electron microscopy (TEM) and spectrophotometer. Then, six plans were designed with different radiation dose values on planning target value. The obtained MRC-5 and MCF-7 cells were treated with non-toxic concentrations of CONPs and then exposed. Finally, cell viability (%) of the cell lines was determined using MTT assay. The findings showed that CONPs have no significant radioprotective effect against 10 cGy radiation dose value. Nevertheless, 70 μM CONPs resulted in a significant radioprotection against 100, 200, 300, 400 and 500 cGy radiation dose values compared with the control group in MRC-5 cells. For all radiation dose values, mean cell viability (%) of MCF-7 had not increased significantly at the presence of nanoceria compared with control group. According to the findings, it was revealed that the use of CONPs have a significant radioprotective effect on normal lung cells, while they do not provide any protection for MCF-7 cancer cells. These properties can help to increase therapeutic ratio of radiotherapy.

Introduction

Cancer is considered as the main cause of death in developed countries and the second chief cause of death in developing countries [1]. Along with chemotherapy and surgery, radiation therapy is used, an important modality, in cancer treatment. It has been reported that approximately 50% of all patients with localized malignancy are treated with radiation therapy [2,3]. The main goal of this treatment modality is to deliver the highest radiation dose to the tumour tissue and the lowest radiation dose to the normal tissue [4]. Tolerability of normal tissues to a radiation dose is limited and a high dose of radiation may cause early and late complications [5]. Generally, there are two main methods to reduce radiation damage caused by radiation therapy, including non-pharmacological and pharmaceutical strategies. The non-pharmacological method is a change in the technique of radiation energy transfer in the tumour. With regard to the emergence of cross-sectional images (CT, MRI, and PET) and modern radiotherapy (IMRT, VMAT, SBRT and IGRT), the correctness and precision of treatments have increased [6–9]. However, the incidence of secondary cancer following radiotherapy is still remarkable and its incidence increases with the advancement of treatment technology [10]. In pharmaceutical strategies, radioprotectors and radiosensitizers are used as a moderator of free radical damage in the targeted radiotherapy [11]. Pharmaceutical strategies may reduce toxicity in normal tissues, leading to reducing normal tissue complications and secondary cancer probability.

Free radicals are responsible for main effect of them in irradiated cells. Free radicals are formed by interaction of ionizing radiation with water molecules which results in radiolysis of water. They react with vital macromolecules which cause functional impairment in cell function [12]. So far, the efficacy of various radioprotectors including both natural and chemical agents, and also nanostructures have been investigated to ameliorate radiation toxicity in different cell types [13,14].

Cerium oxide nanoparticles (CONPs) or nanoceria, in addition to having the general characteristics of the radioprotective nanoparticles such as reactive oxygen species (ROS)

scavenging, biocompatibility, lower toxicity and favourable biologic distribution, have the important feature of self-regeneration which makes it possible to use less concentrations of CONPs to have the desired results [15,16]. CONPs consist of Ce (3+) and Ce (4+) and they are converting to each other constantly. Ce_3O_2 scavenge the free radicals and eventually CeO_2 is produced. With regard to the self-regeneration property, CeO_2 will be decomposed during the chemical process and again Ce_3O_2 is produced to scavenge more ROS. The ability of scavenging the free radicals by nanoceria or the biological activity of the nanoceria is determined by the ratio of the amount of Ce (3+) to Ce (4+). Therefore, Ce (3+) is thought of as an active site for scavenging the free radicals [17]. On the other hand, it was reported that secondary lung cancer after second sarcoma have high relative risk in radiation therapy of breast-cancer [18]. Furthermore, human fibroblast lung cells (MRC-5 cells) are the most sensitive to ionizing radiation and under the same conditions of irradiation, these cells compared to other tissues (such as liver, thyroid gland, and skin) will be the most damaged [19]. Therefore, in the current study, radiation dose-reduction factor (DRF) of CONPs for normal lung cells (MRC-5) and MCF-7 Breast-Cancer Cells was estimated. Furthermore, DRF of CONPs for a wide radiation dose range, which are frequently used in radiation therapy of breast cancer, was determined.

Moreover, small fluctuations in delivered radiation dose can lead to tangible biological changes, subsequently it can lead to changes in the probability of deterministic and stochastic damage [20,21]. The precision and correctness of delivered radiation dose of cells in the in-vitro studies is an important challenge. As far as we know, the process of irradiation to the cells is not clear in the past-studies. In the current study, irradiation schedule with designed phantom is unique and this designed phantom can increase the determination accuracy of DRF for CONPs on cells.

Material and methods

CONPs characterization

CONPs (CeO_2, nanoceria) were acquired US Research Nanoparticles. The grain size and morphology of nanoceria were scrutinized by using scanning electron microscopy (SEM, Phenom, Phenom Prox) with a magnification of 20000x (accelerating voltage of 15 kV) and transmission electron microscopy (TEM, ZEISS, LEO 906) with a magnification of 167000x (accelerating voltage of 100 KeV). Energy dispersive spectroscopy (EDS, Phenom, Phenom Prox) in region mode with a resolution of Mn $K_\alpha \le 140$ eV was used to determine CONPs chemical composition. The UV/VIS absorption of CONPs was recorded by spectrophotometer (4802 UV/VIS double beam spectrometer).

Preparation of CONPs suspension

Nanoceria suspension was prepared with distilled water. To optimize suspension dispersivity syringe filter (PVDF, 0.22-micron, Whatman®) was used and ultrasound sonicator (D-78224 Singen/Htw). According to the UV/VIS spectrum of nanoceria, the wavelength of maximum absorption was determined and used for concentration detection of suspensions. To increase the suspension (with 1000 µg/ml concentration) UV/VIS absorption, time of sonication increased after filtration and the absorption was recorded after 24 h.

Splitting of cell lines

The MRC-5 (human fibroblast line, normal cells, derived from lung) and MCF-7 (human epithelial line, cancerous cells, derived from breast) cell lines were prepared from the Iranian biological research centre, and were seeded in DMEM/F12 and DMEM High Glucose medium containing 10% fatal bovine serum plus penicillin antibiotics (100 IU/ml) and streptomycin (100 µg/ml), respectively and incubated in 37 °C with humidified atmosphere of 5% CO_2.

MTT [3-(4, 5-dimethylthiazol-2-yl)-2, 5-diphenyl-tetrazolium bromide] assay

To assess the effect of CONPs on MRC-5 and MCF-7 cell viability, sub confluent cells (20,000 cell/well) were treated for 24 h with different concentrations of CONPs (0, 5, 10, 30, 50, 70, 110, 150, 200, 250 and 300 µM). After treatment with CONPs, the medium of cells was elicited and added 20 µl of MTT solution (5 mg/ml dissolved in PBS) to each well and micro-plates were then incubated for 3 h at 37 °C in a humidified 5% CO2-air mixture. After configuration of formazan crystals, the MTT solution was discarded from the wells without perturbing the formazan precipitate. 100 µl/well dimethyl sulphoxide (Cinagen®, Iran) was added and then vigorously shaken thoroughly for 10 min to intermingle the formazan crystals. The absorbance of each well was measured with a micro ELISA reader (Biotech Instrument Model: Box998) at 570 nm (triplicate).

Phantom design and irradiation set-up

In order to ensure the uniformity of irradiation to the cell lines, the plexiglass phantom (transparent polycarbonate) was designed and built ($40 \times 40 \times 1$ cm^3, 17 pcs). As shown in Figure 1, 10 slabs with 1 cm thickness were placed under the 96-well plate and 5 slabs with 1 cm thickness were placed on top of it. The centres of 11 and 12 slabs were pierced at the size of 96-well plates ($8.5 \times 12.7 \times 2$ cm^3).

According to the irradiation schedule, the image of phantom was provided by the CT simulator (Siemens, AG, Germany) using the thorax protocol in 89 slices and it was transferred to the Prowess Panther version 5.20 (Prowess Inc., Concord, CA, USA) treatment planning system. It should be noted that all wells of 96-well plates were filled with 200 µl of distilled water.

Six plans were designed with different monitor unites (Mus) on the desired phantom. The information of these plans is presented in Table 1. Planning target volume (PTV), seeded cells at the bottom of the 96-well plate, was

contoured on all CT slices. The dose values of 10, 100, 200, 300, 400500 cGy were delivered to the cell lines using of AP/PA plans. The plans were designed such that the entire PTV received 100% of the prescribed dose (Figure 2).

As seen from Table 1, the couch occupancy factor was considered to be 0.04 in the dose calculation for PA beam. To investigate the effect of CONPs' radioprotection, the cells were cultured in 36 wells of centre with non-toxic concentrations of CONPs. The rest of the wells were filled up to 200 µl of distilled water and then exposed (Figure 1).

Expression of data

Cell viability

The percentage of cytotoxicity was calculated by the following equation:

$$Percentage\ of\ cytotoxicity = \left(1 - \frac{A}{B}\right) \times 100$$

Where A is the optical density of target cells co-incubated with CONPs and B is the optical density of control groups. The concentrations of CONPs which resulted in deaths of more than 10% of the cells, were known as toxic concentrations of nanoceria.

In the next step, the percentage of cell survival was determined according to the following equation:

$$Percentage\ of\ cell\ viability = \left(\frac{C}{D}\right) \times 100$$

Where C is optical density of target cells co-cultured with nanoceria which were treated with ionization radiation and D is the optical density of control groups which were exposed to ionization radiation without using the nanoceria.
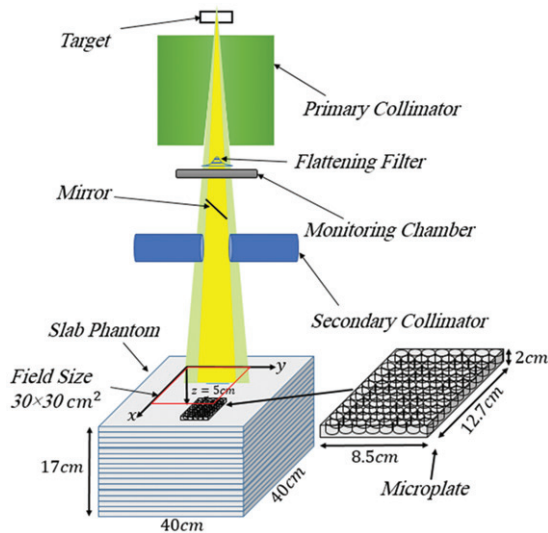

Figure 1. Irradiation set-up of slab phantom. Microplate was placed at a depth of 5 cm from the phantom surface. Cells were cultured in 26 wells of core. In order to prevent the isodose irregularity, the rest of the wells were filled with distilled water.

Table 1. Treatment planning information of slab phantom.

	Beam Data	AP Beam	PA Beam
Common conditions in all Plans	Machine	ONCOR	ONCOR
	Energy	6 MV FP	6 MV FP
	Blocks/MLC	No/No	No/No
	Wedge Name	Open Field	Open Field
	Couch (Lat, Vert, Long) (cm)	0.0, −7.90, 29.50	0.0, −8.10, 29.50
	Isocenter (L-R, I-S, A-P) (cm)	−0.30, 0.00, 0.82	−0.30, 0.00, 1.02
	SSD (cm)	91.1	91.8
	Collimator (°)	0.0	0.0
	Field Size (cm)	30.0 × 30.0	30.0 × 30.0
	Coll Size (cm)	X1:15.0 X2:15.0	X1:15.0 X2:15.0
	Geo. Depth of WP (cm)	Y1:15.0 Y2:15.0	Y1:15.0 Y2:15.0
Plan No.	Prescribed Dose (cGy)	MU/fx	MU/fx
1	10	5.11	5.22
2	100	51.04	52.14
3	200	102.8	104.28
4	300	153.11	156.41
5	400	204.15	208.56
6	500	255.18	260.69

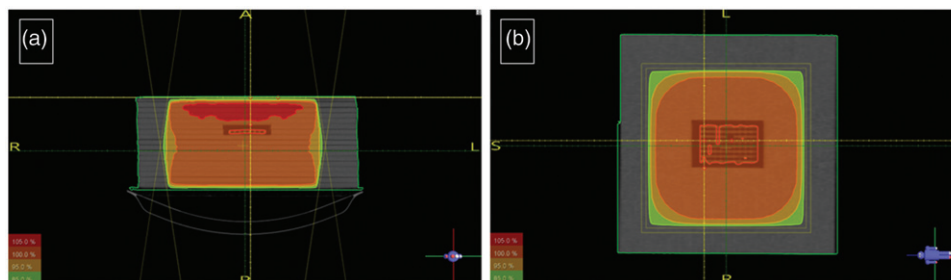All conditions were fixed in the plans, except MU/fx.

Figure 2. Treatment planning by treatment planning system on CT images of phantom. (a) Axial view. (b) Coronal view.
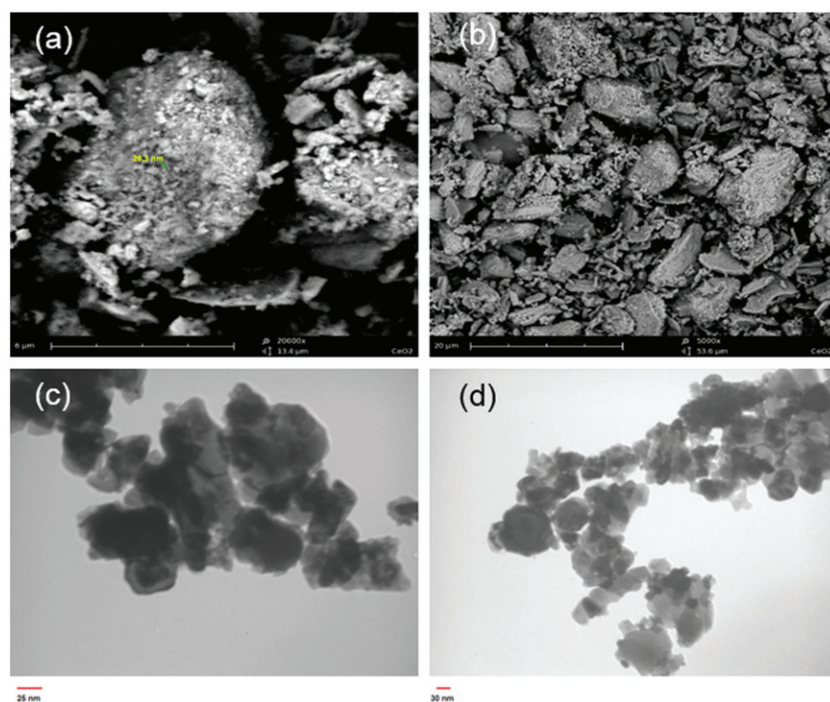
Figure 3. SEM (a and b) and TEM (c and d) images of the CeO_2 nanoparticles at different magnifications.

Dose-reduction factor

The radiation DRF for each cell line treated with CONPs was determined from the general equation at two cell viability percentages (63% and 50%):

$$DRF_{63} = \frac{LD_{63} \; drug \; group}{LD_{63} \; control \; group}$$
$$DRF_{50} = \frac{LD_{50} \; drug \; group}{LD_{50} \; control \; group}$$

Where LD_{63} (lethal dose, 37%) and LD_{50} (lethal dose, 50%) are the radiation dose values that cause the death of 37% and 50% of cells, respectively [22].

Statistical analysis

The data are presented as mean ± standard error of mean. Statistical significances were evaluated using One-way ANOVA, followed by Tukey's multiple comparison *post hoc* test. The 95% confidence level was considered as the statistical significance level of the results.

Results and discussion

Morphology study

The morphological structure of CeO_2 nanoparticles scrutinized by SEM and TEM, as reported in Figure 3. The SEM image of CONPs) Figure 3(a,b) (exhibits that the prepared powders were polygon clusters (with ∼1.5–10 μm sizes) containing nanoparticles (with 29.3 nm sizes). The TEM photographs (Figure 3(c,d)) also approved the presence of the polygon grains (with ∼25–50 nm sizes) in cluster structure. According to the Figure 4, the EDS analysis in region mode
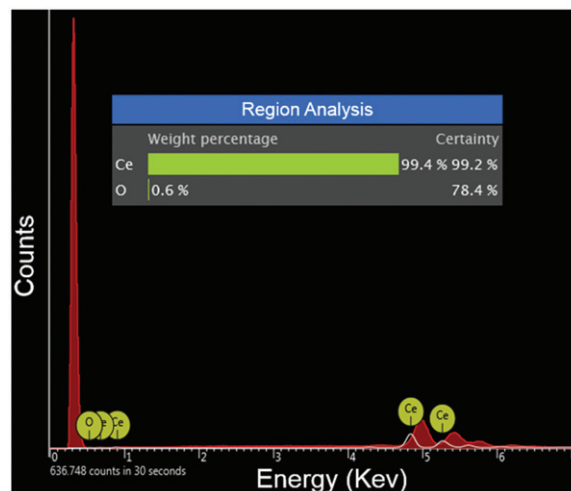

Figure 4. Energy-dispersive X-ray spectrum of CeO_2 nanoparticles.

indicates that a large weight percentage of nanoceria is the cerium element (99.5 wt%).

Optimization of CONPs dispersivity

As seen from the UV/VIS spectrum of CONPs (Figure 5), the maximum UV/VIS absorption of nanoceria was obtained at 318 nm. This wavelength is closely matched with other studies [23,24]. Furthermore, UV/VIS absorption of CONPs suspension (with 1000 μg/ml concentration) is 1.5639 at 318 nm wavelength immediately after preparation. This value with 1 h sonication of nanoceria suspension decreased to 1.0439 after 24 h from stoke fixation; but, 2 h sonication cause that it increased to 1.4694. Eventually, sonication of nanoceria suspension for 2 h led to stable distribution after 24 h from stoke fixation and only 6.04% of the initial concentration of
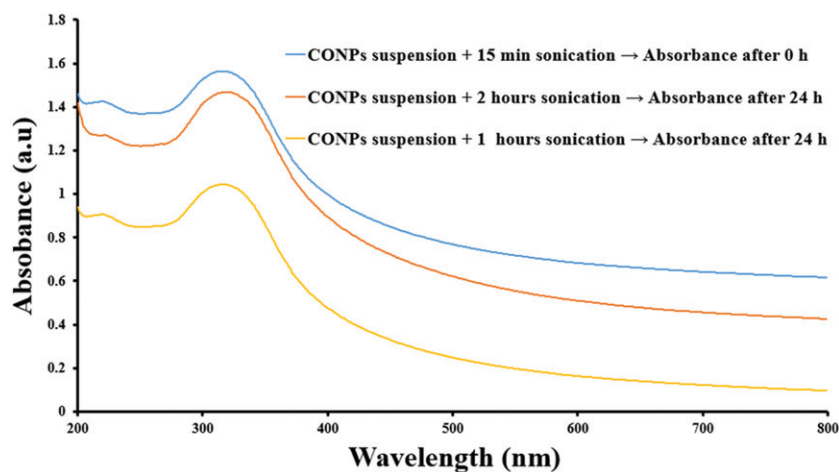
Figure 5. Absorption spectrum of CONPs with different dispersivity plan. The highest absorption was recorded at 318 nm wavelengths.
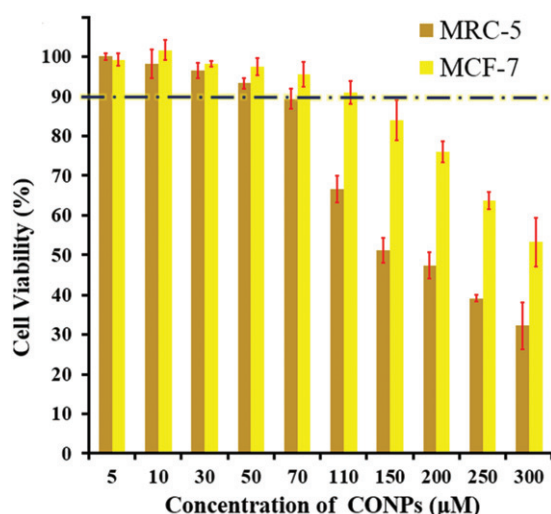

Figure 6. Cell viability (%) of MRC-5 and MCF-7 cell lines for determination of CONPs cytotoxicity. The non-toxic concentration of CONPs was 70 μM.

suspension reduced due to the agglomeration of the nanoceria. With regard to the dispersivity results (Figure 5), all of the suspensions were prepared with 2 h sonication.

Effect of CONPs pretreatment on cell viability

Before evaluating the radioprotective effect of nanoceria, the cytotoxicity of various concentrations of nanoceria was indicated by the MTT assay. In MRC-5 cell lines treated with 5, 10, 30, 50 and 70 μM of nanoceria, cell viability was more than 90% (Figure 6). Because of protecting the normal cells, these concentrations were used to survey the radioprotective effect of CONPs. The toxicity of nanoparticles has been investigated in various studies [16,25–27]. The non-toxic concentration of CONPs can be vary depending on the different conditions such as cell line, nanoparticle synthesis method, and cell viability assay.

Radioprotective effect of cerium oxide nanoparticles

Both cell lines were treated with 5, 10, 30, 50 and 70 μM concentrations of nanoceria and exposed to 6 MV photon beam with different radiation dose values. With regard to the findings of

the MTT assay and statistical analysis (Figure 7), CONPs had no significant radioprotective effect in the both cell lines against 10 cGy radiation dose value (p values >0.05). Therefore, the using of nanoceria in this radiation dose value cannot be justified in observing the radiation protection effects.

Figure 8 presents the experimental data on exposed cells with 100 cGy radiation dose value. In this radiation dose value, treated normal cells with 70 μM of CONPs compared to 0, 5, 10 and 30 μM treatment groups showed a significant increase in the mean cell viability (%) (p values are 0.001, 0.002, 0.003 and 0.012, respectively). Also, 50 μM of nanoceria led to a significant increase in cell viability (%) compared to treatment groups at 0, 5 and 10 μM concentrations of CONPs (p values are 0.013, 0.025, and 0.037, respectively).

The findings of current study (Figure 8) reveal that increasing the CONPs concentration from 50 to 70 μM cannot give rise to significant radioprotection of the normal cells against 100 cGy radiation dose value. Therefore, a 50 μM of nanoceria can be a proper choice for optimal radioprotection against 100 cGy radiation dose value. It is noteworthy that radioprotective effect can be valuable at low concentrations of nanoceria (due to lower toxicity), because the cytotoxicity and disposal mechanism of nanoparticles are very important in this type of applications, especially for heavy nanostructures with high aggregation velocities [28].

As seen from Figure 9, for 200 cGy radiation dose value, there is a significant increment of mean cell viability (%) for MRC-5 cells at the presence of 70 μM of CONPs compared to those of 0, 5, 10, and 30 μM (p values are 0.001, 0.002, 0.001 and 0.005, respectively).

Figure 10 shows that 70 μM of nanoceria can cause to significant protection of normal cells against 300 cGy radiation dose value compared to control group and treatment group with 5 μM of nanoceria (p values are 0.009 and 0.019 respectively). The cancerous cell lines at the presence of nanoceria were not protected against 300 cGy radiation dose value.

According to the statistical analysis (Figure 11), mean cell viability (%) of treatment MRC-5 cells with 70 μM of nanoceria increased significantly compared to the control group and treatment groups with 5, 10 and 30 μM of nanoceria against 400 cGy radiation dose value (p values are 0.002, 0.002, 0.011 and 0.027 respectively).
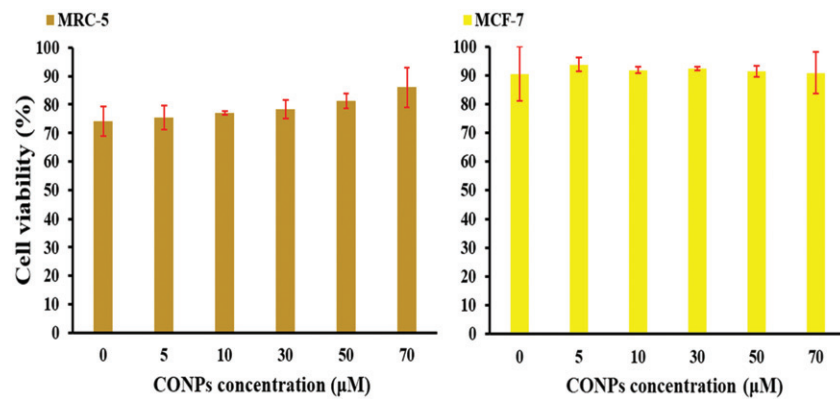
Figure 7. MTT assay was used to measure cell viability (%) of MRC-5 and MCF-7 for determination of radioprotective effect of CONPs. The cells were irradiated with 6 MV X-rays at 10 cGy radiation dose value in the presence of non-toxic concentration of CONPs. Mean ± STD of three-independent experiments ($n = 9$).
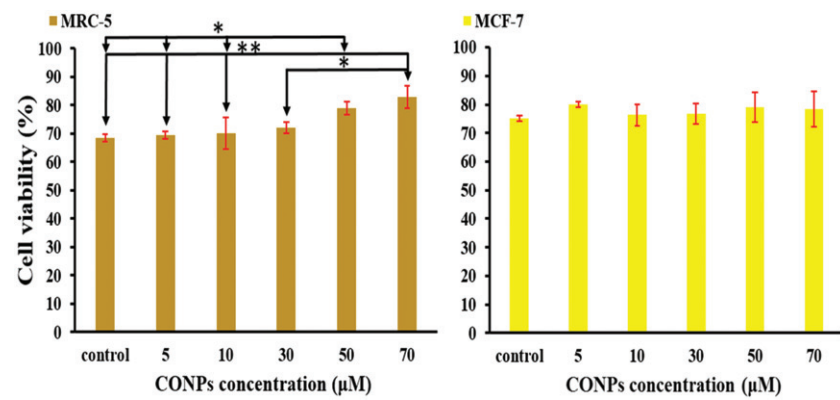

Figure 8. MTT assay was used to measure cell viability (%) of MRC-5 and MCF-7 for determination of radioprotective effect of CONPs. The cells were irradiated with 6 MV X-rays at 100 cGy radiation dose value in the presence of non-toxic concentration of CONPs. Mean ± STD of three-independent experiments ($n = 9$). The groups labeled with * and ** have $p < .01$ and $p < .001$, respectively.
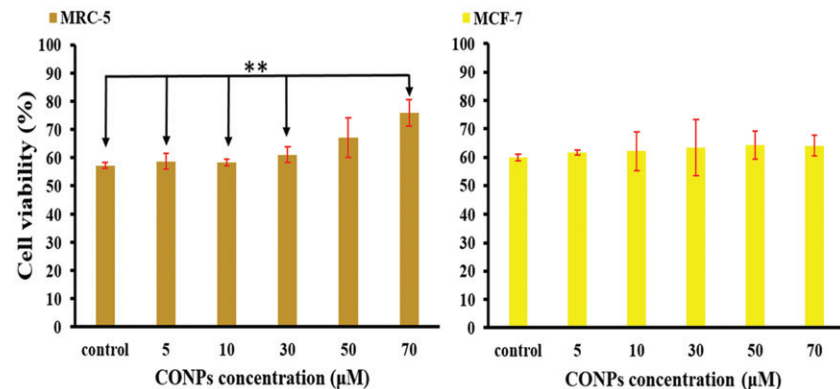

Figure 9. MTT assay was used to measure cell viability (%) of MRC-5 and MCF-7 for determination of radioprotective effect of CONPs. The cells were irradiated with 6 MV X-rays at 200 cGy radiation dose value in the presence of non-toxic concentration of CONPs. Mean ± STD of three-independent experiments ($n = 9$). The groups labeled with ** have $p < .001$.

Figure 12 presents that the normal cells were protected significantly against 500 cGy radiation dose value by 70 µM of nanoceria. Nevertheless, in the cancer cells no protection against radiation by nanoceria occurred.

It is widely reported that CONPs protect normal cells/tissues against ionization radiation. The main reason of these observations is ability of CONPs in scavenging of free radicals [29,30]. Our experiment is in line with previous results [31,32]. Tarnuzzer et al. evaluated radioprotective effect of CONPs on CRL8798, an immortalized normal breast epithelial cell line, and MCF-7 at a 10 Gy radiation dose value. Their results demonstrated that 0.01 µM of these nanoparticles results in the survival of 99% the normal cells after 24 h, while they did not observe any radioprotective effects on cancerous cells. However, there was no reference to type and energy of radiation beam, and irradiation process was also not clear [33]. Briggs et al. and Colon et al. observed radioprotective effect of 145.34 µM and 10 nM concentrations of CONPs on 9 L and CCL 135 cells against different X-ray beams respectively [34,35]. It is notable that different radiation
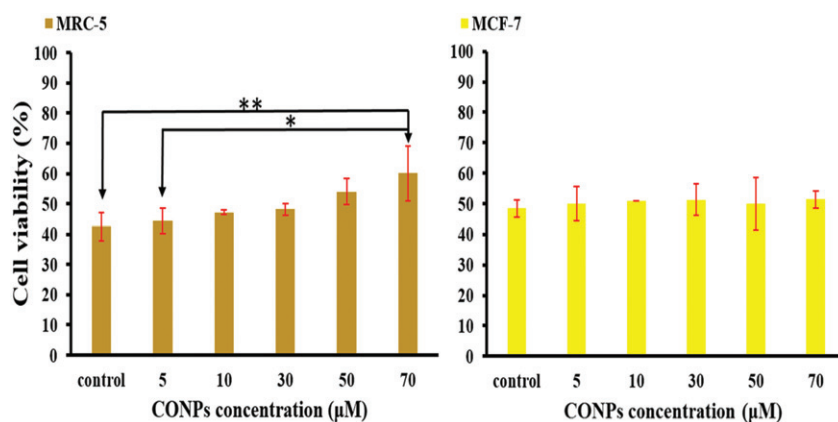
Figure 10. MTT assay was used to measure cell viability (%) of MRC-5 and MCF-7 for determination of radioprotective effect of CONPs. The cells were irradiated with 6 MV X-rays at 300 cGy radiation dose value in the presence of non-toxic concentration of CONPs. Mean ± STD of three-independent experiments ($n = 9$). The groups labeled with * and ** have $p < .01$ and $p < .001$, respectively.
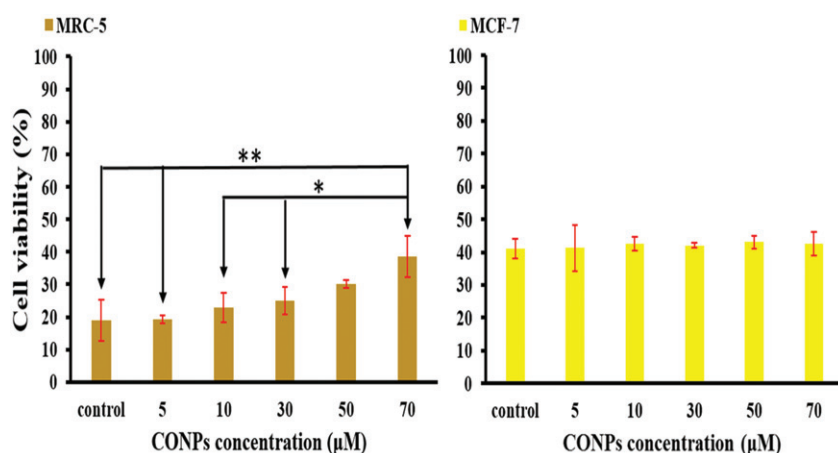

Figure 11. MTT assay was used to measure cell viability (%) of MRC-5 and MCF-7 for determination of radioprotective effect of CONPs. The cells were irradiated with 6 MV X-rays at 400 cGy radiation dose value in the presence of non-toxic concentration of CONPs. Mean ± STD of three-independent experiments ($n = 9$). The groups labeled with * and ** have $p < .01$ and $p < .001$, respectively.
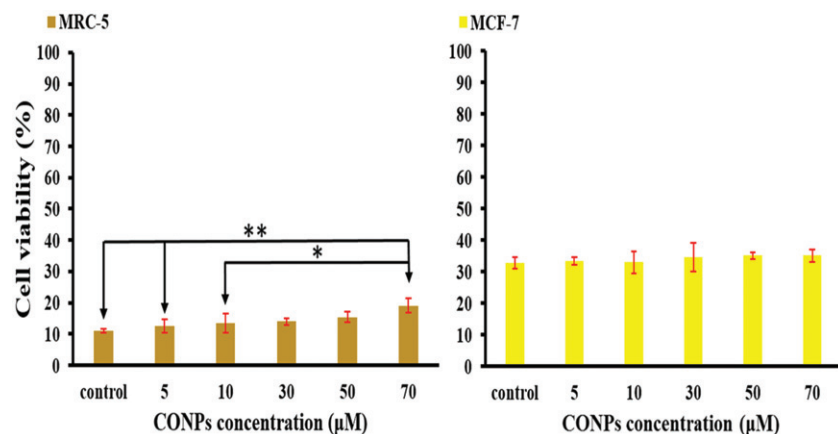

Figure 12. MTT assay was used to measure cell viability (%) of MRC-5 and MCF-7 for determination of radioprotective effect of CONPs. The cells were irradiated with 6 MV X-rays at 500 cGy radiation dose value in the presence of non-toxic concentration of CONPs. Mean ± STD of three-independent experiments ($n = 9$). The groups labeled with * and ** have $p < .01$ and $p < .001$, respectively.

beams have different energy transfer mechanisms, and small variations in delivered dose to cells can lead to large biological changes [21]. The radiation energy and dose value, cell line type, nanoceria suspension preparation schedule and cell viability assay in this current study were different from the above-mentioned studies, which can be the reasons for the difference in observations.

Another finding of the current study (Figure 13) demonstrates that the mean cell viability (%) of normal cells is reduced by the increasing the radiation dose value. Nevertheless, the dose-response pattern of normal cells reveals that the presence of nanoceria can give rise to protection of these cells against ionizing radiation.
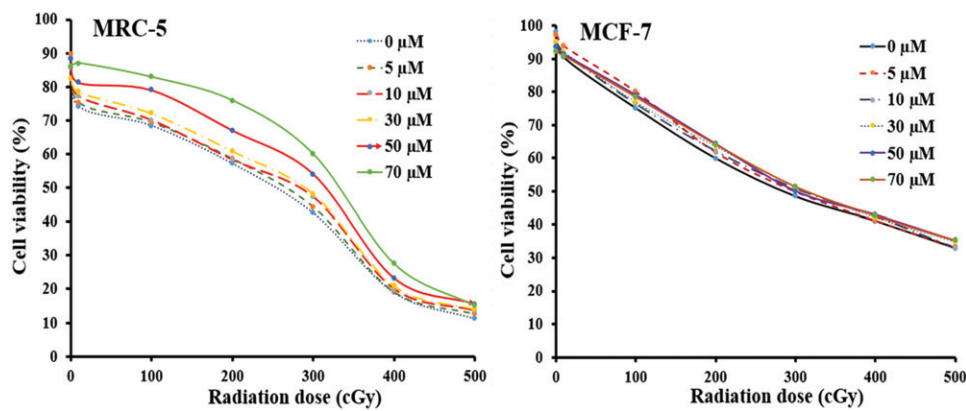
Figure 13. Dose-Response diagrams of MRC-5 and MCF-7 Cell lines in the presence of non-toxic concentration of CONPs.
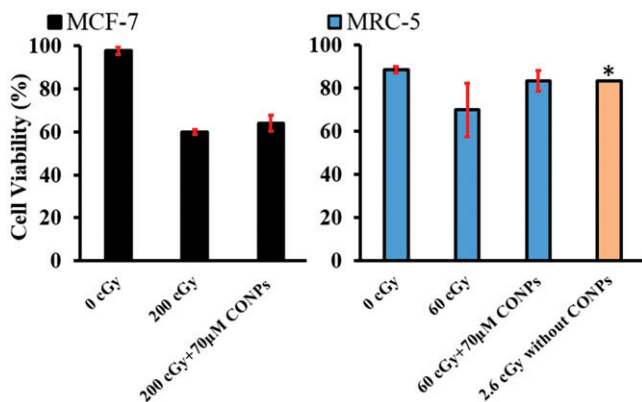

Figure 14. Treatment of cancerous cells with a 200 cGy radiation dose value. Normal cells received 30% of it (60 cGy). The group labeled with * have same cell viability (%) with groups that treated 60 cGy +70 μM CONPs.

On the other hand, the results (Figures 7, 8, 9, 10, 11 and 12) show that presence of CONPs cannot lead to radioprotective effects in cancerous cell line which it can be due to the high rate of proliferation of the cancer cells compared to the normal cells. In the other words, it can be pointed out that CONPs have selective radioprotection effects [31,35].

One of the duties of an oncologist is the reduction of secondary cancer following radiation therapy by appropriate treatment planning. To achieve this goal, it is necessary to know the absorbed dose of cells/tissues. In accordance with the general guidelines in the treatment planning of radiation therapy, when the lung tissue is an organ at risk, its mean that radiation dose should not be greater than 20 to 23 Gy during treatment or 20% lung volume should not receive 30 to 35% of the prescribed radiation dose value. In breast cancer radiation therapy, at 25–30 fractions, cancerous cells will receive 50 Gy radiation dose value [36]. Furthermore, it was reported that if lung tissue receives a 1750 cGy radiation dose during a cancer radiation therapy, the patient will suffer from lung inflammation with a 5% probability after 5 years of treatment. If the radiation dose of lung tissue reaches 2450 cGy, the probability of lung inflammation will be 50% during the same period of time. In the other words, with an increase of 700 cGy in the absorbed dose of lung tissue, the probability of lung inflammation will increase by 45% [37]. Therefore, if the MCF-7 cancerous cells receive a radiation dose of 2 Gy per fraction, in the worst-case conditions, the

MRC-5 cells should not be given a radiation dose of more than 60 cGy (2 cGy ×30% of the prescribed radiation dose value), conditions which were investigated in the current study. According to Figure 14, the mean cell viability (%) of MRC-5 in the group of 60 cGy +70 μM of CONPs is 83.39%. Dose-response curve (Figure 13) shows that a radiation dose value of 2.6 cGy in the absence of CONPs leads to a cell viability of 89.83%. To be more precise, when the lung tissue receives a 1500 cGy radiation dose value during 25 fractions (60 cGy ×25), the presence of 70 μM nanoceria can lead to a biological effect of 65 cGy (2.6 cGy ×25) which it can reduce the risk of inflammation and pulmonary fibrosis significantly.

DRF estimation

Dose-reduction factor (DRF) was calculated for each cell line in 63 and 50% cell viability (using of dose-response curves in Figure 13). According to Figures 15 and 16, there were no increase in DRF_{63} and DRF_{50} values with increment of CONPs concentration in the MCF-7 cell lines. So, the mean DRF value clearly indicated that the nanoceria does not protect cancerous cells against X-ray photon beams. Nevertheless, the mean DRF_{63} value at the presence of 5 μM of nanoceria in the MCF-7 cell lines (1.0815 ± 0.0294) had a higher value than the MRC-5 cell lines at the same concentration of nanoceria (0.99 ± 0.1836) and according to the independent-samples T Test analysis, this difference was significant. Therefore, using of 5 μM of nanoceria cannot be justified to protect the MRC-5 cell lines against 6 MV photon beams.

According to Figure 15, it is apparent that the MRC-5 cell lines at 70 μM of nanoceria had been protected significantly compared to the 5, 10 and 30 μM of nanoceria (p values are 0.001, $p < 0.001$ and $p < 0.005$, respectively). Also, the statistical analysis of results revealed that DRF_{63} value at 50 μM of nanoceria (1.4596 ± 0.1580) than 10 μM (1.1100 ± 0.1821) has been increased in MRC-5 cell lines. Hence, 50 μM of nanoceria can be a good choice to observe radioprotective effect in the MRC-5 cell lines, because of lower toxicity in this concentration of nanoceria (Cell death $=6.63\%$) than 70 μM (Cell death $=10.6\%$).

According to the DRF_{50} values in Figure 16, the normal cells have not been protected by nanoceria significantly. On the basis of the data above, it is possible to predict that 70 μM of
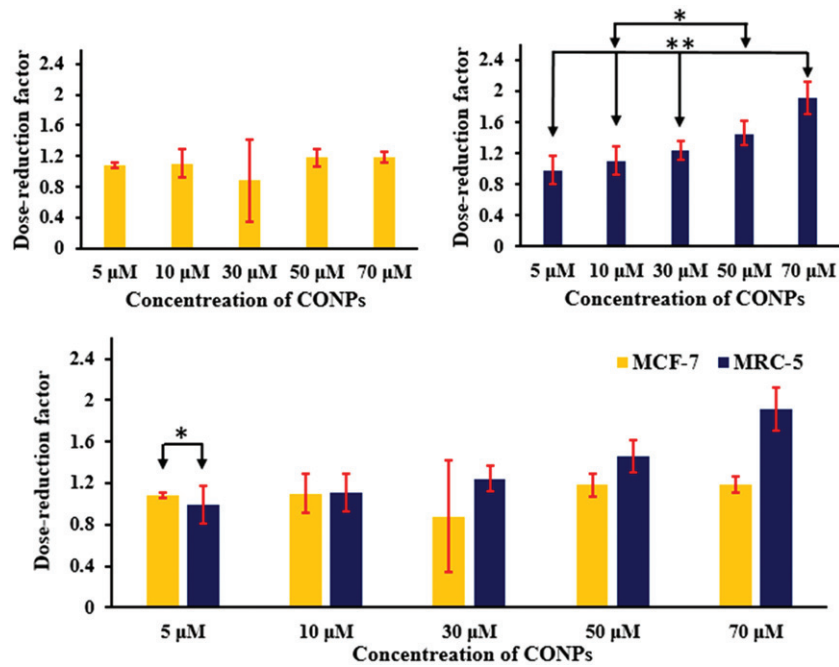
Figure 15. DRF$_{63}$ of CONPs in MRC-5 and MCF-7 cell lines against 6 MV photon beams.
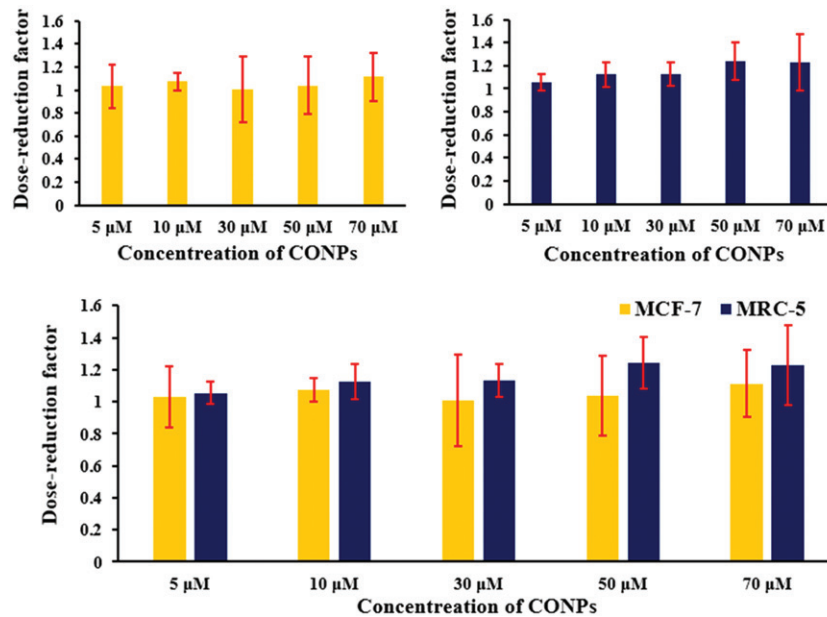

Figure 16. DRF$_{50}$ of CONPs in MRC-5 and MCF-7 cell lines against 6 MV photon beams.

nanoceria contribute to significant radioprotective effect in the normal cells when radiation inhibited the 37% of cells, without having a specific plan for targeted drug delivery. As far as we know, very few research studies have calculated the DRF for nanoceria. In a study by Ouyang et al., it was reported that that DRF value increases with increment of nanoceria concentration. However, this factor decreased with the increment of radiation energy form 40 kVp to 140 kVp [30].

Perspective of future research

Th current study could be a springboard for more investigation on estimating the DRF value of CONPs in other cell lines with various radiation energy and dose values. Moreover, it is clear that the quantification of radioprotection or radiosensitization effects is correct when the absorbed radiation dose by target should be accurate. In this study, it was attempted to design a unique phantom for accurate delivery of radiation dose to target. As a future study, suggestion of a better method than the current study would be of interest.

Conclusions

The findings of the current study reveal that the using of CONPs in radiation therapy (with higher radiation dose values) can have a significant radioprotective effect on the MRC-5 normal cells. Using of nanoceria at the 70 μM concentration can increase the viability of normal cells by 14.45,

18.76, 17.52, 19.66 and 7.93% against 100, 200, 300, 400 and 500 cGy of 6 MV photon beams, respectively. Nonetheless, it cannot protect the MCF-7 cell lines against X-ray beams. Particularly when the nanocarriers are not as tissue-targeted drug delivery systems, it can be certain that the cancerous tissues are not significantly protected by CONPs against X-ray beams. Because cancerous cells have a high proliferation, and Ce_3O_2 cannot scavenge the countless free radicals induced by radiation in this tissue. As a result, it can be mentioned that at the equal concentrations of CONPs, the active site of Ce (3+) in normal cells are higher than those of cancerous cells.

Acknowledgements

Disclosure statement

No potential conflict of interest was reported by the authors.

References

[1] Farhood B, Geraily G, Alizadeh A. Incidence and mortality of various cancers in Iran and compare to other countries: a review article. Iran J Public Health. 2018;47:309–316.

[2] Yahyapour R, Motevaseli E, Rezaeyan A, et al. Reduction-oxidation (redox) system in radiation-induced normal tissue injury: molecular mechanisms and implications in radiation therapeutics. Clin Transl Oncol. 2018;20:975–988.

[3] Bahreyni Toossi MT, Soleymanifard S, Farhood B, et al. Assessment of accuracy of out-of-field dose calculations by TiGRT treatment planning system in radiotherapy. J Cancer Res Ther. 2018;14:634–639.

[4] Baskar R, Lee KA, Yeo R, et al. Cancer and radiation therapy: current advances and future directions. Int J Med Sci. 2012;9:193–199.

[5] Kumar S. Second malignant neoplasms following radiotherapy. Ijerph. 2012;9:4744–4759.

[6] Supramaniam R. New malignancies among cancer survivors: SEER cancer registries, 1973–2000. J Epidemiol Community Health. 2008;62:375–376.

[7] Bertelsen A, Hansen CR, Johansen J, et al. Single arc volumetric modulated arc therapy of head and neck cancer. Radiother Oncol. 2010;95:142–148.

[8] Small WJR. Image-Guided Radiation Therapy. In: Youl M, Brock KK, Dawson LA (eds). Clinical Radiation Oncology: Indications, Techniques, and Results. Hoboken, NJ: John Wiley & Sons, Inc; 2017. p. 83–98.

[9] Khan FM, Gibbons JP. Khan's the Physics of Radiation Therapy. Philadelphia: Lippincott Williams & Wilkins; 2014.

[10] Sountoulides P, Koletsas N, Kikidakis D, et al. Secondary malignancies following radiotherapy for prostate cancer. Ther Adv Urol. 2010;2:119–125.

[11] Velpula N, Ugrappa S, Kodangal S. A role of radioprotective agents in cancer therapeutics: a review. Int J Basic Clin Pharmacol. 2013;2:677–682.

[12] Farhood B, Goradel NH, Mortezaee K, et al. Intercellular communications-redox interactions in radiation toxicity; potential targets for radiation mitigation. J Cell Commun Signal. 2018; (in press).

[13] Najafi M, Motevaseli E, Shirazi A, et al. Mechanisms of inflammatory responses to radiation and normal tissues toxicity: clinical implications. Int J Radiat Biol. 2018;94:335–356.

[14] Yahyapour R, Shabeeb D, Cheki M, et al. Radiation protection and mitigation by natural antioxidants and flavonoids; implications to radiotherapy and radiation disasters. Cmp. 2018;11:285–304.

[15] Niu J, Wang K, Kolattukudy PE. Cerium oxide nanoparticles inhibit oxidative stress and nuclear factor-κB activation in H9c2 cardiomyocytes exposed to cigarette smoke extract . J Pharmacol Exp Ther. 2011;338:53–61.

[16] Pešić M, Podolski-Renić A, Stojković S, et al. Anti-cancer effects of cerium oxide nanoparticles and its intracellular redox activity. Chem Biol Interac. 2015;232:85–93.

[17] Baker CH. Harnessing cerium oxide nanoparticles to protect normal tissue from radiation damage. Transl Cancer Res. 2013;2:343–358.

[18] Grantzau T, Overgaard J. Risk of second non-breast cancer after radiotherapy for breast cancer: a systematic review and meta-analysis of 762,468 patients. Radiother Oncol. 2015;114:56–65.

[19] Valentin J. The 2007 Recommendations of the International Commission on Radiological Protection. Amsterdam: Elsevier Oxford; 2007.

[20] Andreassi MG, Piccaluga E, Gargani L, et al. Subclinical carotid atherosclerosis and early vascular aging from long-term low-dose ionizing radiation exposure: a genetic, telomere, and vascular ultrasound study in cardiac catheterization laboratory staff. JACC Cardiovas Interv. 2015;8:616–627.

[21] Hall EJ, Giaccia AJ. Radiobiology for the Radiologist. Philadelphia: Lippincott Williams & Wilkins; 2006.

[22] Nadi S, Monfared AS, Mozdarani H, et al. Effects of arbutin on radiation-induced micronuclei in mice bone marrow cells and its definite dose reduction factor. Iran J Med Sci. 2016;41:180–185.

[23] Yin L, Wang Y, Pang G, et al. Sonochemical synthesis of cerium oxide nanoparticles-effect of additives and quantum size effect. J Colloid Interface Sci. 2002;246:78–84.

[24] Goharshadi EK, Samiee S, Nancarrow P. Fabrication of cerium oxide nanoparticles: characterization and optical properties. J Colloid Interface Sci. 2011;356:473–480.

[25] Lin W, Huang Y-w, Zhou X-D, et al. Toxicity of cerium oxide nanoparticles in human lung cancer cells. Int J Toxicol. 2006;25:451–457.

[26] Park E-J, Choi J, Park Y-K, et al. Oxidative stress induced by cerium oxide nanoparticles in cultured BEAS-2B cells. Toxicology. 2008;245:90–100.

[27] Rubio L, Annangi B, Vila L, et al. Antioxidant and anti-genotoxic properties of cerium oxide nanoparticles in a pulmonary-like cell system. Arch Toxicol. 2016;90:269–278.

[28] Bystrzejewska-Piotrowska G, Golimowski J, Urban PL. Nanoparticles: their potential toxicity, waste and environmental management. Waste Manag. 2009;29:2587–2595.

[29] Colon J, Hsieh N, Ferguson A, et al. Cerium oxide nanoparticles protect gastrointestinal epithelium from radiation-induced damage by reduction of reactive oxygen species and upregulation of superoxide dismutase 2. Nanomedicine. 2010;6:698–705.

[30] Ouyang Z, Mainali MK, Sinha N, et al. Potential of using cerium oxide nanoparticles for protecting healthy tissue during accelerated partial breast irradiation (APBI). Phys Med. 2016;32:631–635.

[31] Goushbolagh NA, Farhood B, Astani A, et al. Quantitative cytotoxicity, cellular uptake and radioprotection effect of cerium oxide nanoparticles in MRC-5 normal cells and MCF-7 cancerous cells. Bionanosci. 2018;8:769–777.

[32] Popov A, Zaichkina S, Popova N, et al. Radioprotective effects of ultra-small citrate-stabilized cerium oxide nanoparticles in vitro and in vivo. RSC Adv. 2016;6:106141–106149.

[33] Tarnuzzer RW, Colon J, Patil S, et al. Vacancy engineered ceria nanostructures for protection from radiation-induced cellular damage. Nano Lett. 2005;5:2573–25737.

[34] Briggs A, Corde S, Oktaria S, et al. Cerium oxide nanoparticles: influence of the high-Z component revealed on radioresistant 9L cell survival under X-ray irradiation. Nanomedicine. 2013;9:1098–1105.

[35] Colon J, Herrera L, Smith J, et al. Protection from radiation-induced pneumonitis using cerium oxide nanoparticles. Nanomedicine. 2009; 5:225–231.

[36] Khan FM, Gerbi BJ. Treatment Planning in Radiation Oncology. Philadelphia: Wolters Kluwer Health/Lippincott Williams & Wilkins; 2012.

[37] Emami B, Lyman J, Brown A, et al. Tolerance of normal tissue to therapeutic irradiation. Int J Radiat Oncol Biol Phys. 1991;21: 109–122.